# Orthogonal PbS Nanowire Arrays and Networks and Their Raman Scattering Behavior

**Jian-Ping Ge,[a] Jin Wang,[a] Hao-Xu Zhang,[a, b] Xun Wang,[a] Qing Peng,[a] and Ya-Dong Li*[a]**

**Abstract:** Three-dimensional, orthogonal lead sulfide (PbS) nanowire arrays and networks have been prepared by using a simple, atmospheric pressure chemical vapor deposition (APCVD) method. These uniform nanowires (average diameter 30 nm) grow epitaxially from the surface of the initial PbS crystal seeds and form orthogonal arrays and networks in space. The growth mechanism has been explored, and the process was classified as homogeneous, epitaxial growth in the ⟨200⟩ directions. Furthermore, Raman spectra of PbS nanowires are reported here, and their characteristic Raman peak (190 $cm^{-1}$, no shoulder) could be used as a unique probe for the study of PbS nanomaterials.

**Keywords:** chemical vapor deposition · crystal growth · nanostructures · Raman spectroscopy

## Introduction

Recently, one-dimensional (1D) nanostructures have become the focus of intense research, because they provide a good system to investigate the dependence of electrical, optical, and thermal transport or mechanical properties on dimensionality and size confinement. In 1998, Lieber and co-workers reported a laser ablation method for synthesizing crystalline semiconductor nanowires[1] and made a series of attempts to assemble these nanowires into functional structures.[2] Based on that successful preparation, various kinds of prototype nanodevices, such as biological nanosensors,[3] logic gates,[4] and address decoders,[5] have been developed. Later, Yang and co-workers synthesized self-organized, ⟨0001⟩-oriented zinc oxide nanowire arrays,[6] which were confirmed to be the first nanolasers acting under optical excitation. This structure was also used as a template for the "epitaxial casting" approach to single-crystal gallium nitride (GaN)[7] and silicon (Si)[8] nanotube arrays. At the same time, the nanoribbon structure, a distinctly different but general 1D nanostructure, was discovered by Wang et al.,[9] further enriching the family of nanoscale building blocks.

In the past few years, nanowires have been developed from uniform structures to ones which have their composition and doping modulated along the axial[10] and radial[11] directions, and are being developed towards branched structures.[12] Even more applications and new functions might emerge if these 1D nanocrystals could be synthesized in shapes of higher complexity than the single-shaped ones (wires, rods, and tubes) produced by current methods.[13–18]

Herein we report the synthesis of a three-dimensional, orthogonal lead sulfide (PbS) nanowire array, a nanostructure building block, as well as PbS nanowire networks with various shapes, by means of a simple, atmospheric pressure chemical vapor deposition (APCVD) method. The intended product, PbS, because of its unique properties as a π–π semiconductor with a small band gap (0.41 eV) and a large exciton Bohr radius (18 nm),[19] has been extensively studied in solar cells,[20] electroluminescence,[21] photoluminescence,[22] and mode-locking in lasers.[23]

Various methods have been used to fabricate PbS crystals. In the early 1970s, PbS whiskers about 400 μm long and 140 μm wide were synthesized by heating PbS at 800 °C in a vacuum chamber.[24] These crystals could also be obtained by the reaction of sulfur and lead in liquid ammonia at

[a] J.-P. Ge, J. Wang, Dr. H.-X. Zhang, Dr. X. Wang, Dr. Q. Peng, Prof. Y.-D. Li
Department of Chemistry and the Key Laboratory of Atomic & Molecular Nanosciences (Ministry of Education, China)
National Center for Nanoscience and Nanotechnology
Tsinghua University, Beijing 100084 (P. R. China)
Fax: (+86) 106-278-8765
E-mail: ydli@mail.tsinghua.edu.cn

[b] Dr. H.-X. Zhang
Nanoscale Physics & Devices Laboratory
Institute of Physics, Chinese Academy of Science
Beijing 100080 (P. R. China)

Supporting information for this article is available on the WWW under http://www.chemeurj.org/ or from the author.

 **DOI: 10.1002/chem.200400633**  

room temperature.[25] Recently, with the development of nanoscience and nanotechnology, more and more interest has been focused on the production of PbS nanoparticles and nanowhiskers. Uniform cube-shaped PbS nanocrystals (<10 nm) were produced by mixing metal-oleylamine complexes with sulfur at 220 °C.[26] Larger particles (~50 nm) were prepared by sintering the precursor in aerosols.[27] Even microorganisms were used to yield nanocrystals (~5 nm).[28] With respect to nanowhiskers, most approaches involve solutions, such as the synthesis of PbS dendrites,[12] nanowires,[29] and PbS nanostructures inside mesoporous silica.[14] However, few reports refer to the gas-phase route.

Our synthesis was based on the chemical vapor deposition process between sulfur and metal chlorides under atmospheric pressure.[30–32] A furnace with a horizontal quartz tube was employed for the synthesis reactions. Lead chloride ($PbCl_2$) powder was placed in a ceramic boat in the middle of the furnace, where the temperature could be exactly measured and adjusted, and sulfur (S) powder was positioned upstream of this. Under flowing argon, after heating at about 650–750 °C for 2 h, the products were deposited on the (100) silicon wafer placed at the downstream end of the furnace. The specific parameters for the various samples are listed in Table 1. The as-deposited products

Table 1. Specific experimental parameters for the synthesis of various samples.[a]

| Sample | Furnace temperature [°C] | Substrate location [cm] | Substrate temperature [°C] | Ar flow rate [sccm] | Morphology |
|---|---|---|---|---|---|
| 1 | 650 | 11 | 520 | 100 | array/wire |
| 2 | 650 | 11 | 520 | 150 | array/wire |
| 3 | 650 | 11–12 | 520–450 | 100 | wires |
| 4 | 750 | 11 | 620 | 100 | networks |
| 5 | 650 | 13–14 | 380–340 | 50 | seeds |
| 6 | 700 | 13–14 | 450–410 | 100 | seeds |

[a] The synthesis run time for each sample was 120 min.

were characterized and analyzed (see the Experimental Section for details) by X-ray diffraction (XRD), scanning electron microscopy (SEM), transmission electron microscopy (TEM), high-resolution TEM (HRTEM), energy-dispersive X-ray spectroscopy (EDS), and Raman spectroscopy.

## Results and Discussion

**Epitaxial growth of PbS arrays**: The SEM images in Figures 1a and b show a typical as-prepared unit of a PbS nanowire array (sample 1), which was deposited on a (100) silicon wafer that had been placed 11 cm away from the center of the furnace. The SEM image reveals that the construction of this unique unit consists of six bundles of well-aligned PbS nanowires and an obvious cubic crystal seed. The cube is about 1 to 3 μm in size, and the length of the nanowires reaches 10 μm. Each nanowire bundle is perfectly perpendicular to its neighboring ones within the same seed, and they seem to grow out of the cube surface, which suggests that the process might be classified as homogeneous, epitaxial growth.

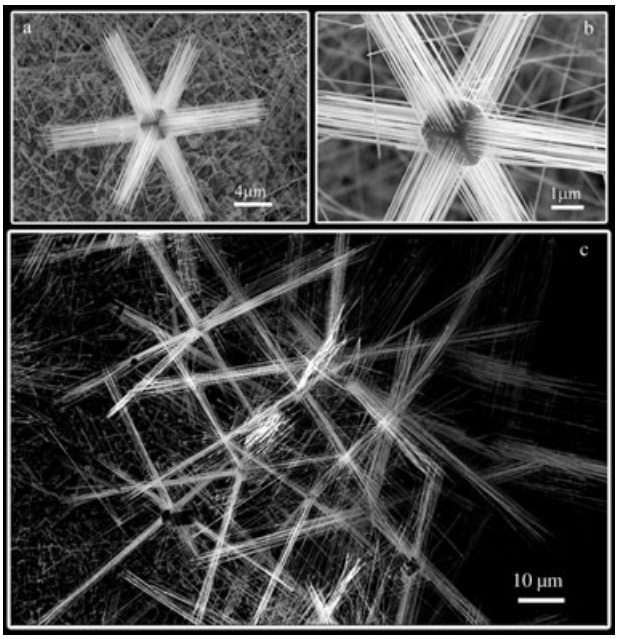


Figure 1. a) and b) SEM images of the three-dimensional nanowire array with an observable cubic seed; c) SEM image of units of the nanowire arrays prepared under a larger gas flow rate.

A key parameter for adjusting the size of this unit is the proper concentration of the source materials, which is mainly determined by the carrier gas flow rate in our preparations. Figure 1c shows the morphology of the array units (sample 2) prepared with the same parameters as Figures 1a and b, but with a different flow rate. On increasing the flow rate (from 100 to 150 sccm), the lengths of the nanowire arms range from 10 to 40 μm, which illustrates that a greater flow rate will favor whisker growth.

**PbS nanowires**: We also obtained large amounts of PbS nanowires (sample 3, Figure 2) tens of micrometers in length by using very similar experimental parameters. The as-prepared nanowires could be classified as either of two species. Nanowires deposited at a higher temperature ($T=520$ °C) are usually hard and straight, whereas those deposited at a lower temperature ($T=450$ °C) are generally soft and curved. This evident difference may be due to the different growth rates in different temperature zones.

TEM images of individual nanowires provide further insight into the structure of these materials. The nanowires have a typical diameter of 30 nm (Figure 2d). To verify the crystal characteristics and growth direction, a HRTEM image of a PbS nanowire is given in Figure 2e, which shows that the wire is structurally uniform and consists of a single crystal. The crystal surface of the face-centered cubic (fcc) PbS nanowire has been indexed by means of the electron diffraction (ED) pattern (Figure 2e, inset), and it was found

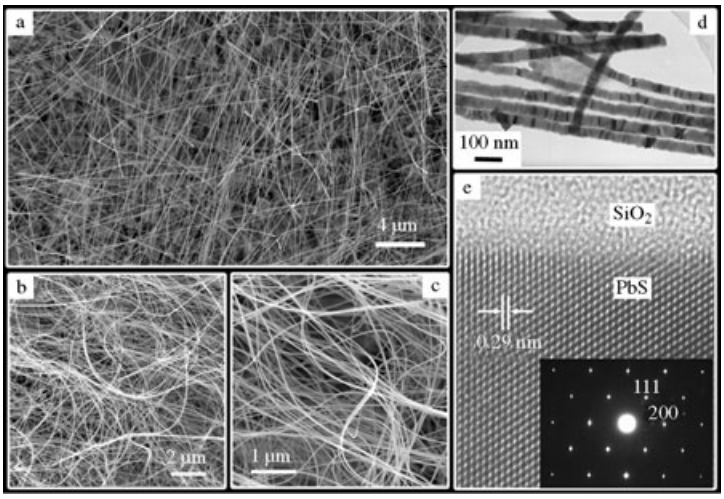


Figure 2. a)–c) SEM and d) TEM images of straight and curved PbS nanowires. e) A HRTEM image showing that the wire grows in the ⟨200⟩ direction. The inset shows the ED pattern taken parallel to the [02$\bar{2}$] axis.

that the ⟨200⟩ direction is parallel to the wire axis. The HRTEM image exhibits well-resolved (200) lattice planes, and the experimentally measured lattice spacing ($0.29 \pm 0.01$ nm) is consistent with the 0.2966 nm separation in bulk crystals (JCPDS No. 78–1058), which again confirms the growth direction of the as-prepared nanowire.

XRD patterns of the substrate covered with PbS nanowires without further treatment after preparation were measured (Supporting Information, Figure 1). All peaks could be indexed by a fcc-structured PbS crystal with a lattice constant of $a = 5.93$ Å, consistent with the standard values for bulk PbS (JCPDS No. 78–1058). No peaks due to any other phases were detected, and only the presence of Pb and S atoms were detected by EDS analysis, all of which indicated that the nanowires were highly pure and well crystallized.

**PbS nanowire networks with various shapes**: When the temperature of the furnace was raised to 750 °C, we obtained several kinds of PbS nanowire networks (sample 4) with different shapes, such as sphere, octahedron (hexapod whiskers; Figure 3), and pyramids (tri- and tetrapod whiskers; Figure 4). The typical size of the network was in the range of 20 to 30 μm, and the straight nanowires present were highly oriented in three-dimensional space.

Although the shapes are very different, all of the networks have the same characteristic: the nanowires are parallel or perpendicular to each other, forming an orthogonal nanowire network in three-dimensional space. Taking spherical networks as an example, the average diameter of the sphere is about 20 μm (Figure 3a), and the whole network consists of a large amount of uniform nanowires. A high-resolution SEM image (Figure 3b) shows that the nanowires grow strictly along the *x*, *y*, and *z* axes. Each nanowire is parallel or perpendicular to the one nearby, exhibiting high orientation. The same phenomenon appears in the other networks.

It is interesting that the orthogonal morphology is a common structural characteristic for the samples (samples 1, 2, and 4) prepared under similar conditions. How does this orthogonal unit grow?

**Growth process and mechanism**: Before discussing the formation of the orthogonal array of nanowires and their networks, we should first study the "crystal seeds" deposited far away from the center of the furnace (Position B; see Figure 2 in the Supporting Information) relative to the nanowires formed at the center (Position A). When the temperature of the furnace rises, the temperatures of Positions A and B rise. At any point in time, Position B has the same temperature as that which Position A had previously, due to the temperature

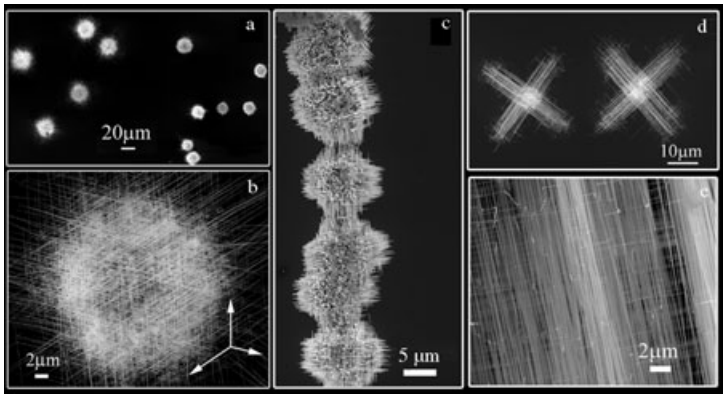


Figure 3. a) and b) Spherical and c)–e) octahedral-shaped orthogonal PbS nanowire networks.

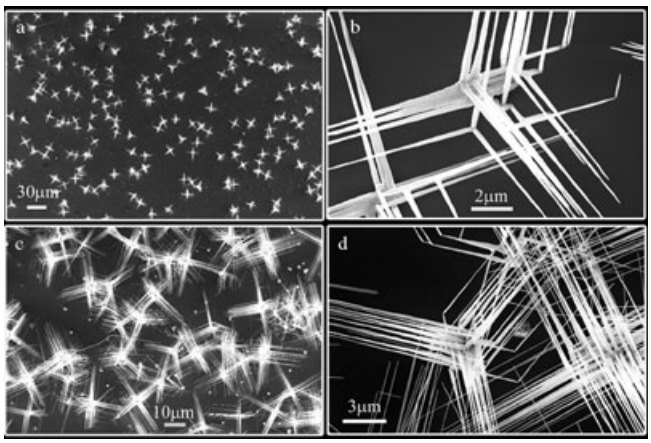


Figure 4. Examples of pyramidal-shaped orthogonal PbS nanowire networks.

  

profile of the furnace. If the direction of the gas flow and a sufficient supply of the source material are considered, samples collected at Position B might have formed earlier at Position A; this relationship may be helpful to better understand the growth process. Therefore, these crystal seeds formed at Position B were also collected for observation.

Two kinds of crystal seeds were obtained in the low-temperature zone (Position B). The first one was prepared at a furnace temperature of 650 °C. It has an almost completely cubic morphology, and has nanowire pillars growing out of every crystal face of the cubic seed (sample 5, Figure 5). It is

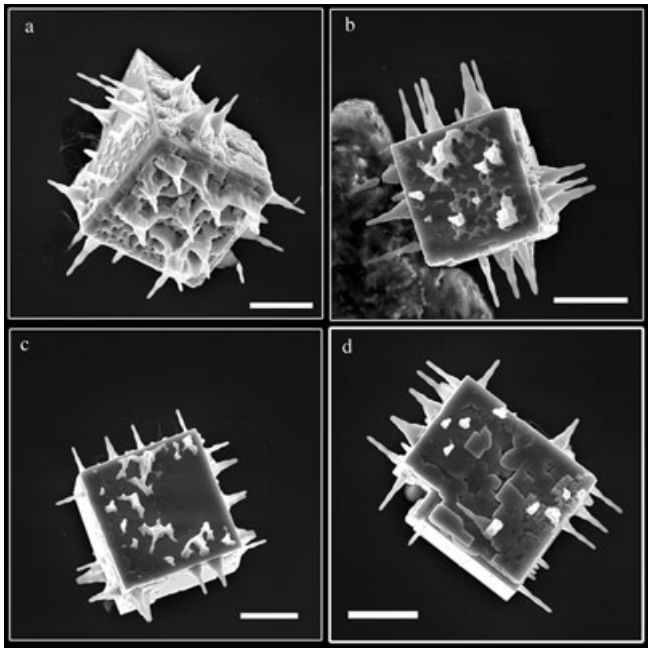


Figure 5. A cubic crystal seed displaying balanced growth of nanopillars from all surfaces. The bars in each picture represent 1 μm.

conceivable that with a temperature rise and sufficient supply of source material, the seed would gradually turn into an array unit described above. However, the amount of this kind of seed or the corresponding array unit was not very large, because accurate control is needed for the formation of a perfect crystal seed and its balanced growth in every direction. In most cases, irregular seeds and unbalanced growth led to all kinds of nanowire orthogonal networks. Figure 6 shows these irregularly shaped crystal seeds (sample 6), which were generally found in every experiment carried out under similar conditions . These seeds always had an irregular shape, and nanopillars only grew along three to four of the six orthogonal directions. It is suggested that they might be the original form of the PbS nanowire networks.

Combining the study of the growth direction and the analysis of the crystal seeds, the process should be classified as homogeneous, epitaxial growth due to crystal growth in the

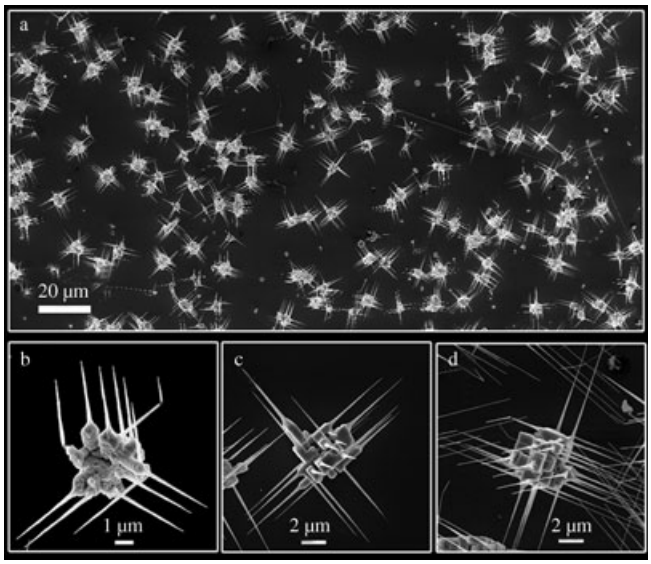


Figure 6. Irregularly shaped seeds with unbalanced growth of nanopillars.

six equivalent directions of ⟨200⟩. Consider the nanowire array unit, for example (Figure 7). In the first step, evaporated S and $PbCl_2$ form a small cubic seed several micrometers in size, which has quite a lot of defects in its surface (Fig-

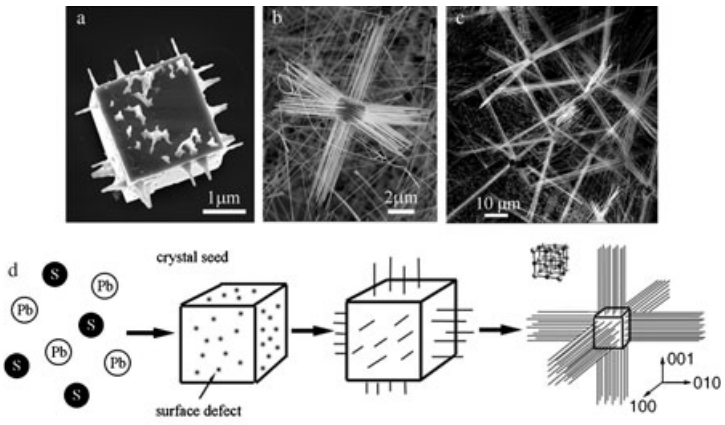


Figure 7. a)–c) The different stages of the growth process and d) a schematic flow diagram of these stages.

ure 7a). During the reaction process, the concentration of the source material decreases to a low level, favoring crystal growth as long whiskers. The surface defects might serve as the active sites for the initial growth, and uniform PbS nanowires grow perpendicularly out of the seed surface. As the cubic seed has six equivalent faces (200, 020, 002, …), and the nanowire grows in the ⟨200⟩ direction, this process should be classified as homogeneous, epitaxial growth. Only a perfectly cubic crystal seed (Figure 5) and balanced growth in the six equivalent directions brings the typical nanowire morphology; while any disturbance, such as irregular seed shape and unbalanced growth (Figure 6), may lead to the orthogonal networks with various shapes.

**Raman scattering of PbS nanowires**: It is well known that in a crystalline semiconductor the observed Raman shifts usually correspond to the longitudinal optical phonons (LO), whereas, other modes, such as the transverse optical phonons (TO) and the surface phonons (SP), are, in general, not observable because of symmetry restrictions and low intensities, respectively. However, as the surface-to-volume ratio is large for nanostructured materials, it is possible to observe the SP mode by Raman scattering measurements.[33–34] The surface roughness as well as the crystal size also play important roles in modifying the Raman spectra. Therefore, Raman scattering has become a unique probe for the study of nanomaterials. As no reports on the Raman properties of PbS nanowires have appeared to date, we carried out some preliminary studies to enrich the available knowledge of the properties of this nanomaterial.

Raman scattering measurements were performed at room temperature (300 K) using the $Ar^+$-ion laser with an excitation wavelength of 514.5 nm. The Raman scanning spectrometer is equipped with a charge-coupled device (CCD) detector. A typical Raman spectrum of the PbS nanowires with 5 mW laser power is shown in the lower half of Figure 8. According to earlier reports,[35–37] Raman peaks at

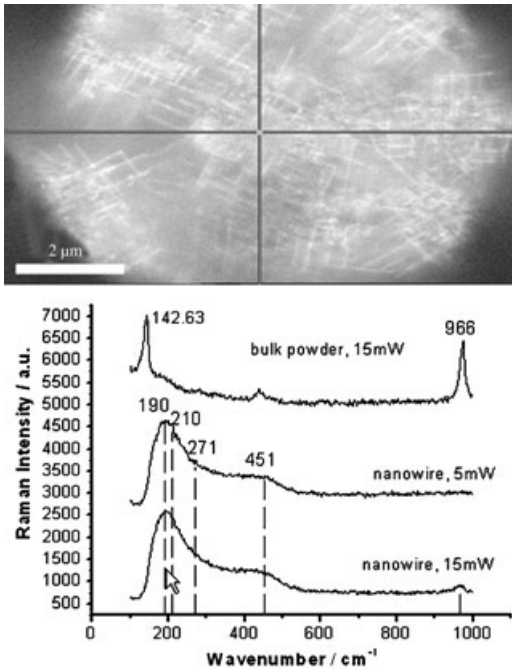


Figure 8. An optical image of the PbS nanowires recorded by a CCD detector (top), and Raman spectra obtained at different laser powers (bottom).

210, 271, and 451 $cm^{-1}$ should be observed, corresponding to a 1 LO phonon mode, a two-phonon process, and a 2 LO phonon mode, respectively. In addition, the peak or shoulder at ~190 $cm^{-1}$ has been identified to be due to the SP mode, and its intensity greatly increases with decreasing crystal size.

In our results, one strong peak at 190 $cm^{-1}$ and one shoulder at 451 $cm^{-1}$ are clearly observed. The Raman peak due to the SP mode is so intense that the peaks at 210 and 271 $cm^{-1}$ become two small shoulders, which are difficult to characterize. This phenomenon discloses a unique property of PbS nanowire: the strongest Raman scattering peak appears at 190 $cm^{-1}$. For PbS nanocrystals, only shoulders at 190 and 205 $cm^{-1}$ were observed, corresponding to 1.5 nm and 18 nm nanocrystals, respectively.

When the laser power was increased to 15 mW, one peak at 966 $cm^{-1}$ appeared due to the photodegradation of PbS. It should be a characteristic peak for the oxidation products $PbSO_4$, $PbO{\cdot}PbSO_4$, $3\,PbO{\cdot}PbSO_4$, and $4\,PbO{\cdot}PbSO_4$. The following reactions (Equations (1)–(5)) have been proposed upon referring to an earlier report.[38] We also measured the Raman spectra of bulk PbS powders under the same testing conditions. The bulk PbS powders were prepared by a simple precipitation reaction between $Pb(CH_3COO)_2$ and $Na_2S$, followed by an annealing process at 573 K. Only Raman peaks at 142, 451, and 966 $cm^{-1}$ were observed, which is quite different from the results for PbS nanocrystals and nanowires.

$$PbS \xrightarrow{h\nu,\ O_2} \alpha\text{-}PbO + SO_2 \uparrow \quad (1)$$

$$PbS \xrightarrow{\alpha\text{-}PbO,\ O_2} PbSO_4 \quad (2)$$

$$\alpha\text{-}PbO + PbSO_4 \rightarrow PbO \cdot PbSO_4 \quad (3)$$

$$3\,\alpha\text{-}PbO + PbSO_4 \rightarrow 3\,PbO \cdot PbSO_4 \quad (4)$$

$$4\,\alpha\text{-}PbO + PbSO_4 \rightarrow 4\,PbO \cdot PbSO_4 \quad (5)$$

## Conclusion

In the future, it would be worth adding further structural complexity to the nanocrystal family of building blocks, as well as investigating their relationship to a nanowire structure.[39] Herein we report the synthesis of a PbS nanocrystal building block by means of a simple, APCVD method. Detailed research into the intrinsic growth characteristics of the PbS crystal suggests that many useful semiconductor materials having a cubic structure, such as PbSe, ZnSe, CdSe, and GaN, might also be fabricated to give the same shape as the PbS nanowires synthesized here. With proper assembly, these unique structures might serve as special connection parts or optoelectric transformation parts in nanoscale devices of electronic and photonic transportation. Raman spectra of PbS nanowires are, for the first time to our knowledge, reported here, and the characteristic peak (not a shoulder) at 190 $cm^{-1}$ could be used as a unique tool for the study of PbS nanomaterials.

  

## Experimental Section

**Materials**: Lead chloride ($PbCl_2$) was prepared by the simple precipitation reaction between sodium chloride (NaCl) and lead nitrate ($Pb(NO_3)_2$). All reagents used in this work, including NaCl, $Pb(NO_3)_2$, and sulfur powder, were A. R. reagents (>99.99%) from the Beijing Chemical Factory, China, and were used as-received without any treatment. Single-crystal (100) silicon (Si) wafers were cleaned prior to use by washing with ethanol and subsequently drying in air.

**Synthesis**: Our crystal growth apparatus consisted of a furnace with a horizontal quartz tube. The temperature profile was measured previously to determine the deposition temperature. $PbCl_2$ powder (1 mM) held in a ceramic boat was placed in the middle of the furnace, where the temperature could be exactly measured and adjusted. Sulfur powder (0.4 g) was placed upstream, and the (100) Si wafer was located downstream of the boat. The temperature was raised to a particular value by using a heating rate of 10 K min$^{-1}$ under flowing argon and remained at that point for 2 h. The furnace was cooled down to room temperature slowly (about 5 K min$^{-1}$), and the products were deposited on the Si substrate.

**Characterization**: The samples were characterized by using a Bruker D8 Advance X-ray diffractmeter with $Cu_{K\alpha}$ radiation ($\lambda = 1.5418$ Å). The size and morphology of the as-prepared PbS nanowires were examined by using a Hitachi Model H-800 transmission electron microscope, a LEO 1530 scanning electron microscope, and a JEOL JEM-2010F high-resolution transmission electron microscope. EDS was also carried out with the transmission electron microscopes. Raman spectra were recorded with an RM2000 microscopic confocal Raman spectrometer (Renishaw, England), which had a 514 nm laser beam and a charge coupled device detector with a 4 cm$^{-1}$ resolution. The spectra were obtained by a 1–2 μm laser spot being focused on the sample.

## Acknowledgements

This work was supported by NSFC (90406003, 20401010, 50372030, 20025102, 20131030), the Foundation for the Author of National Excellent Doctoral Dissertation of P. R. China, and the state key project of fundamental research for nanomaterials and nanostructures (2003CB716901).

[1] A. M. Morales, C. M. Lieber, *Science* **1998**, *279*, 208.
[2] Y. Huang, X. F. Duan, Q. Q. Wei, C. M. Lieber, *Science* **2001**, *291*, 630.
[3] Y. Cui, Q. Q. Wei, H. Park, C. M. Lieber, *Science* **2001**, *293*, 1289.
[4] Y. Huang, X. F. Duan, Y. Cui, L. J. Lauhon, K. H. Kim, C. M. Lieber, *Science* **2001**, *294*, 1313.
[5] Z. H. Zhong, D. L. Wang, Y. Cui, M. W. Bockrath, C. M. Lieber, *Science* **2003**, *302*, 1377.
[6] M. H. Huang, S. Mao, H. Feick, H. Q. Yan, Y. Y. Wu, H. Kind, E. Weber, R. Russo, P. D. Yang, *Science* **2001**, *292*, 1897.
[7] J. Goldberger, R. He, Y. F. Zhang, S. Lee, H. Q. Yan, H. J. Choi, P. D. Yang, *Nature* **2003**, *422*, 599.
[8] R. Fan, Y. Y. Wu, D. Y. Li, M. Yue, A. Majumdar, P. D. Yang, *J. Am. Chem. Soc.* **2003**, *125*, 5254.
[9] Z. W. Pan, Z. R. Dai, Z. L. Wang, *Science* **2001**, *291*, 1947.
[10] M. S. Gudiksen, L. J. Lauhon, J. F. Wang, D. C. Smith, C. M. Lieber, *Nature* **2002**, *415*, 617.
[11] L. J. Lauhon, M. S. Gudiksen, D. L. Wang, C. M. Lieber, *Nature* **2002**, *420*, 57.
[12] D. Kuang, A. Xu, Y. Fang, H. Liu, C. Frommen, D. Fenske, *Adv. Mater.* **2003**, *15*, 1747.
[13] W. S. Shi, H. Y. Peng, Y. F. Zheng, N. Wang, N. G. Shang, Z. W. Pan, C. S. Lee, S. T. Lee, *Adv. Mater.* **2000**, *12*, 134.
[14] F. Cao, Q. Y. Lu, X. Y. Liu, Y. S. Yan, D. Y. Zhao, *Nano Lett.* **2001**, *1*, 743.
[15] X. G. Peng, L. Manna, W. D. Yang, J. Wickham, E. Scher, A. Kadavanich, A. P. Alivisatos, *Nature* **2000**, *404*, 59.
[16] S. Wang, S. Yang, *Langmuir* **2000**, *16*, 389.
[17] Y.-D. Li, J. W. Wang, Z. X. Deng, Y. Y. Wu, X. M. Sun, D. P. Yu, P. D. Yang, *J. Am. Chem. Soc.* **2001**, *123*, 9904.
[18] E. Leontidis, M. Orphanou, T. K. Leodidou, F. Krumeich, W. Caseri, *Nano Lett.* **2003**, *3*, 569.
[19] J. L. Machol, F. W. Wise, R. C. Patel, D. B. Tanner, *Phys. Rev. B* **1993**, *48*, 2819.
[20] R. Plass, S. Pelet, J. Krueger, M. Gratzel, U. Bach, *J. Phys. Chem. B* **2002**, *106*, 7578.
[21] L. Bakueva, S. Musikhin, M. A. Hines, T. W. F. Chang, M. Tzolov, G. D. Scholes, E. H. Sargent, *Appl. Phys. Lett.* **2003**, *82*, 2895.
[22] N. O. Dantas, F. Qu, R. S. Silva, P. C. Morais, *J. Phys. Chem. B* **2002**, *106*, 7453.
[23] G. Tamulaitis, V. Gulbinas, G. Kodis, A. Dementjev, L. Valkunas, I. Motchalov, H. Raaben, *J. Appl. Phys.* **2000**, *88*, 178.
[24] A. R. Patel, K. Sangwal, *J. Cryst. Growth* **1971**, *8*, 282.
[25] G. Henshaw, I. P. Parkin, G. A. Shaw, *J. Chem. Soc. Dalton Trans.* **1997**, 231.
[26] J. Joo, H. B. Na, T. Yu, J. H. Yu, Y. W. Kim, F. Wu, J. Z. Zhang, T. Hyeon, *J. Am. Chem. Soc.* **2003**, *125*, 11100.
[27] K. K. Nanda, F. E. Kruis, H. Fissan, M. Acet, *J. Appl. Phys.* **2002**, *91*, 2315.
[28] M. Kowshik, W. Vogel, J. Urban, S. K. Kulkarni, K. M. Paknikar, *Adv. Mater.* **2002**, *14*, 815.
[29] D. Yu, D. Wang, Z. Meng, J. Lu, Y. Qian, *J. Mater. Chem.* **2002**, *12*, 403.
[30] J. P. Ge, Y.-D. Li, *Chem. Commun.* **2003**, 2498.
[31] J. P. Ge, Y.-D. Li, *Adv. Funct. Mater.* **2004**, *14*, 157.
[32] J. P. Ge, J. Wang, H. X. Zhang, Y.-D. Li, *Chem. Eur. J.* **2004**, *10*, 3525.
[33] A. Mlayah, A. M. Brugman, R. Carles, J. B. Renucci, M. Ya. Valakh, A. V. Pogorelov, *Solid State Commun.* **1994**, *90*, 567.
[34] K. K. Nanda, S. N. Sahu, *Appl. Surf. Sci.* **1997**, *119*, 50.
[35] T. D. Krauss, F. W. Wise, D. B. Tanner, *Phys. Rev. Lett.* **1996**, *76*, 1376.
[36] T. D. Krauss, F. W. Wise, *Phys. Rev. B* **1997**, *55*, 9860.
[37] K. K. Nanda, S. N. Sahu, R. K. Soni, S. Tripathy, *Phys. Rev. B* **1998**, *58*, 15405.
[38] Y. Batonneau, C. Brémard, J. Laureyns, J. C. Merlin *J. Raman Spectrosc.* **2000**, *31*, 1113.
[39] D. L. Wang, C. M. Lieber, *Nat. Mater.* **2003**, *2*, 355.

Received: June 23, 2004
Revised: November 13, 2004
Published online: February 1, 2005